

# The Cosmic Expansion History from Line-Intensity Mapping

José Luis Bernal,<sup>1,2,3</sup> Patrick C. Breyse,<sup>4</sup> and Ely D. Kovetz<sup>5</sup>

<sup>1</sup>*ICC, University of Barcelona, IEEC-UB, Martí i Franquès 1, E08028 Barcelona, Spain*

<sup>2</sup>*Dept. de Física Quàntica i Astrofísica, Universitat de Barcelona, Martí i Franquès 1, E08028 Barcelona, Spain*

<sup>3</sup>*Institut d'Estudis Espacials de Catalunya (IEEC), E08034 Barcelona, Spain*

<sup>4</sup>*Canadian Institute for Theoretical Astrophysics, University of Toronto,  
60 St. George Street, Toronto, ON, M5S 3H8, Canada*

<sup>5</sup>*Department of Physics, Ben-Gurion University, Be'er Sheva 84105, Israel*

Line-intensity mapping (LIM) of emission from star-forming galaxies can be used to measure the baryon acoustic oscillation (BAO) scale as far back as the epoch of reionization. This provides a standard cosmic ruler to constrain the expansion rate of the Universe at redshifts which cannot be directly probed otherwise. In light of growing tension between measurements of the current expansion rate using the local distance ladder and those inferred from the cosmic microwave background, extending the constraints on the expansion history to bridge between the late and early Universe is of paramount importance. Using a newly derived methodology to robustly extract cosmological information from LIM, which minimizes the inherent degeneracy with unknown astrophysics, we show that present and future experiments can gradually improve the measurement precision of the expansion rate history, ultimately reaching percent-level constraints on the BAO scale. Specifically, we provide detailed forecasts for the SPHEREx satellite, which will target the H $\alpha$  and Lyman- $\alpha$  lines, and for the ground-based COMAP instrument—as well as a future stage-3 experiment—that will target the CO rotational lines. Besides weighing in on the so-called Hubble tension, reliable LIM cosmic rulers can enable wide-ranging tests of dark matter, dark energy and modified gravity.

PACS numbers:

Measurements of its expansion history have always been at the heart of our understanding of the Universe. This dates back to Hubble's ninety-year-old discovery of the expansion [1], which marked the dawn of scientific cosmology, to the discovery just twenty years ago that the expansion is currently accelerating [2, 3], which provided the last piece in what is now widely considered to be the standard model of cosmology, known as  $\Lambda$ CDM.

To this date, there are two main observational handles on the expansion rate of the Universe. One relies on calibrating a distance ladder towards standard-candle type-Ia supernovae in our *local* cosmic neighborhood. The other comes from the *distant* early Universe, via the extraction of the baryon acoustic oscillation (BAO) scale, which is robustly determined by the sound horizon at recombination, from cosmic microwave background (CMB) measurements. These opposite handles anchor the so-called direct and inverse distance ladder, respectively [4].

One of the most pressing mysteries in cosmology today is why these measurements have been growing in tension [5]. The tension between the value of  $H_0$  as directly measured in the local Universe [6] and the value inferred from Planck CMB measurements [7] (when  $\Lambda$ CDM is assumed), has surpassed  $4\sigma$  in statistical significance [6, 8]. If real, the discrepancy can be re-framed as a mismatch between the two anchors of the cosmic distance ladder [9]. Low redshift observations [10, 11] strongly constrain the expansion rate of the Universe under the  $\Lambda$ CDM prediction. The difference could be due to modifications in the very early Universe or in the epoch  $3 \lesssim z \lesssim 1000$ , which is too faint to probe with discrete galaxy surveys.

In this *Letter*, we explore how upcoming and future line-intensity mapping (LIM) [12] experiments can bridge

the gap between the local and distant observations to enable the measurement of the full expansion history of the Universe [13]. LIM experiments can achieve this feat as they integrate light from all emitting sources, including the numerous galaxies at high redshift which are too faint to be detected individually. Thus, by targeting bright, easily-identifiable spectral lines and covering a wide range of frequencies with high spectral resolution, LIM can provide tomographic maps of specific line emission across extended epochs in the history of the Universe.

However, a key challenge to the extraction of precise cosmological information from line-intensity maps is the degeneracy with astrophysics, as this line emission is determined by star-formation processes and by both intra and intergalactic gas physics. Unfortunately, these processes are likely never to be understood with the required precision for cosmological analyses. To circumvent this predicament, we will follow a novel methodology—presented in detail in a companion paper [14]—to isolate the cosmological information and optimize its extraction. Encouragingly, we find that next-decade experiments can reach  $\sim 1\%$  constraints on the expansion history over redshifts  $2 \lesssim z \lesssim 6$ , and within 4%-10% error at  $z \lesssim 8$ , providing (robust) invaluable insight on the Hubble tension.

We start by reviewing how the BAO scale can be constrained via measurements of the LIM power spectrum. When transforming redshifts and sky positions into distances to compute a power spectrum, a fiducial cosmology must be assumed. However, the inferred distances will be distorted if the adopted cosmology does not match the correct one [15]. This effect—named after Alcock and Paczynski—is the key to interpreting the measured BAO scale in a cosmological framework as a standard ruler.

In Fourier space, the relation between the true and measured wavenumbers along the line of sight and in the transverse directions is given by  $k_{\parallel}^{\text{tr}} = k_{\parallel}^{\text{meas}}/\alpha_{\parallel}$  and  $k_{\perp}^{\text{tr}} = k_{\perp}^{\text{meas}}/\alpha_{\perp}$ , where the rescaling parameters are defined as:

$$\alpha_{\perp} = \frac{D_A(z)/r_s}{(D_A(z)/r_s)^{\text{fid}}}, \quad \alpha_{\parallel} = \frac{(H(z)r_s)^{\text{fid}}}{H(z)r_s}, \quad (1)$$

where  $D_A(z)$  and  $H(z)$  are the angular diameter distance and the Hubble expansion rate at redshift  $z$ , respectively,  $r_s$  is the sound horizon at radiation drag, and fiducial quantities are denoted by ‘fid’. Measurements of the BAO feature can be compared against the fiducial expectation, providing a direct constraint on  $D_A(z)/r_s$  and  $H(z)r_s$ . An external prior on  $r_s$  can then be applied to infer absolute measurements of the expansion history.

Line-intensity fluctuations provide a biased tracer of the underlying density field (which contains the cosmological information), but are also strongly linked to astrophysical processes. To efficiently separate between the astrophysical and cosmological dependences in the LIM power spectrum, it is useful to group all the degenerate parameters (see Ref. [14] for details) and express it as:

$$P(k, \mu) = \left( \frac{\langle T \rangle b \sigma_8 + \langle T \rangle f \sigma_8 \mu^2}{1 + 0.5 (k \mu \sigma_{\text{RSD}})^2} \right)^2 \frac{P_m(k)}{\sigma_8^2} + P_{\text{shot}}, \quad (2)$$

where  $\mu = \hat{k} \cdot \hat{k}_{\parallel}$  is the cosine of the angle between the mode vector  $\vec{k}$  and  $k_{\parallel}$ . The power spectrum depends on  $\langle T \rangle$ , the expected value of the brightness temperature, the luminosity bias  $b$ , the growth factor  $f$ , and the amplitude  $\sigma_8$  and shape  $P_m(k)$  of the matter power spectrum.  $P_{\text{shot}}$  is the shot-noise power spectrum, and  $\sigma_{\text{RSD}}$  accounts for redshift-space distortions on small scales. Note that we drop the  $z$ -dependence from all quantities to simplify notation. From Eq. (2), the set of parameter combinations that can be directly measured from the LIM power spectrum at each independent redshift bin and observed patch of sky is  $\vec{\theta} = \{\alpha_{\perp}, \alpha_{\parallel}, \langle T \rangle f \sigma_8, \langle T \rangle b \sigma_8, \sigma_{\text{RSD}}, P_{\text{shot}}\}$ .

The multipoles of the observed power spectrum are [14]

$$\begin{aligned} \tilde{P}_{\ell}(k^{\text{meas}}) &= \frac{H(z)}{H^{\text{fid}}(z)} \left( \frac{D_A^{\text{fid}}(z)}{D_A(z)} \right)^2 \frac{2\ell + 1}{2} \times \\ &\times \int_{-1}^1 d\mu^{\text{meas}} \tilde{P}(k^{\text{true}}, \mu^{\text{true}}) \mathcal{L}_{\ell}(\mu^{\text{meas}}), \end{aligned} \quad (3)$$

where  $\mathcal{L}_{\ell}$  is the Legendre polynomial of degree  $\ell$  and the observed power spectrum is determined by the observational window function, using  $\tilde{P}(k, \mu) = W(k, \mu)P(k, \mu)$ .

In this work we focus on spectral lines related to star formation, which are brighter than HI with respect to the corresponding foregrounds, and hence may be more promising to provide higher signal-to-noise measurements of the large-scale structure as far back as the epoch of reionization. In order to model the line intensities, we associate a star-formation rate to a halo of a

given mass, and compute the expected luminosity density and other astrophysical quantities using the halo mass function. We consider Lyman- $\alpha$ , H $\alpha$  and CO(1-0), and follow the models and prescriptions of Refs. [16], [17] and [18], respectively. The standard approach in these models is to use a set of scaling relations (calibrated from simulations and/or dedicated observations) to associate a star-formation rate to a halo of a given mass, and then relate it to the line luminosity. This can then be integrated over the halo mass function to get an expected signal [19–21]. In our analysis below we adopt the fiducial parameter values presented in these works, naively interpolating (or extrapolating) them to other redshifts, as needed. Naturally, herein lies the largest uncertainty in our forecasts. However, we emphasize that our use of Eqs. (2),(3) ensures that the influence of the astrophysical uncertainties is minimal. While in a pessimistic scenario the amplitude of the signal may be lower than we forecast, the marginalization over the astrophysical parameters renders the analysis less susceptible to differences in the shape of the biases or luminosity functions.

To estimate the potential of LIM BAO measurements, we forecast measurements of the following planned and future experiments targeting the spectral lines above:

1. SPHEREx [22]: In addition to performing a wide galaxy survey, SPHEREx will carry out LIM surveys. Launching in 2023, this satellite’s IM missions will target Lyman- $\alpha$  and H $\alpha$  emission, as well as H $\beta$  and the oxygen lines OII and OIII (albeit with lower significance, making them less suitable for cosmological analyses). Specifically, we consider the SPHEREx deep survey, which will cover  $200 \text{ deg}^2$  of the sky with higher sensitivity than the all-sky survey. SPHEREx will have 6.2 arcsec angular resolution at full-width half maximum, and  $R = \nu_{\text{obs}}/\delta\nu = 41.4$  spectral resolution at  $0.75 < \lambda_{\text{obs}} < 4.1 \mu\text{m}$  and  $R = 150$  at  $4.1 < \lambda_{\text{obs}} < 4.8 \mu\text{m}$  (where  $\delta\nu$  is the width of the frequency channel, and  $\nu_{\text{obs}}$  and  $\lambda_{\text{obs}}$  are the observed frequency and wavelength, respectively) [22]. We restrict ourselves to  $0.75 < \lambda_{\text{obs}} < 4.1 \mu\text{m}$ , as that is the H $\alpha$  wavelength range modelled in Ref. [17]. We assume a sensitivity<sup>1</sup> such that the product  $\nu_{\text{obs}}\sigma_N/\sqrt{t_{\text{pix}}} = \{3.04, 1.49, 0.81, 0.61\} \text{ nW/m}^2/\text{sr/pixel}$  for H $\alpha$  at  $\nu_{\text{obs}} = \{29.5, 15.7, 10.9, 8.3\} \times 10^4 \text{ GHz}$ ; and  $\{3.59, 3.15, 2.54\} \text{ nW/m}^2/\text{sr/pixel}$  for Lyman- $\alpha$  at  $\nu_{\text{obs}} = \{36.6, 30.8, 25.2\} \times 10^4 \text{ GHz}$ .

2. COMAP [23]: Already observing, COMAP is a single-dish, ground-based telescope targeting the CO lines in the frequency band 26-34 GHz. The instrument houses 19 single-polarization detectors with an angular resolution of 4 arcmin and channel width of  $\delta\nu = 15.6 \text{ MHz}$ . The expected system temperature is  $T_{\text{sys}} \sim 40 \text{ K}$ . The first phase, COMAP1, will observe for  $t_{\text{obs}} = 6000$  hours with one telescope, while the second phase, COMAP2 will observe for 10000 hours using

<sup>1</sup> Olivier Doré, private communication.

Instrumental Parameter	COMAP 1	COMAP 2	IMS3 (CO)
$T_{\text{sys}}$ [K]	40	40	$\max(20, \nu_{\text{obs}})$
Total # of independent detectors	19	95	1000
Ang. resolution (FWHM) [arcmin]	4	4	4
Frequency band [GHz]	26-34	26-34	12-36
$\delta\nu$ [MHz]	15.6	8.0	2.0
$t_{\text{obs}}$ [h]	6000	10000	10000
$\Omega_{\text{field}}$ [deg <sup>2</sup> ]	2.25	60	1000

TABLE I: Experimental specifications for COMAP1 (under construction), the planned COMAP2, and our IMS3 design.

four additional telescopes, all with an improved spectral resolution of  $\delta\nu = 8$  MHz. We assume a sky coverage of  $\Omega_{\text{field}} = 60$  deg<sup>2</sup> for COMAP2, which optimizes the significance of the power spectrum measurement.

3. IMS3 (CO): Finally, we envision a next generation (or stage 3) of LIM experiments—IMS3, in short. We conceive of a ground-based CO experiment as an upgrade of COMAP, and assume it will integrate over the frequency range 12-36 GHz for 10000 hours. Based on Refs. [24, 25], we assume  $T_{\text{sys}} = \max[20, \nu_{\text{obs}} (\text{K}/\text{GHz})]$ . We compare the experimental specifications of both COMAP phases and the IMS3 CO experiment in Table I.

To track the evolution of the signal, we divide the observed volumes into redshift bins (except for the case of COMAP). We consider in each case non-overlapping, independent redshift bins such as  $\log_{10}[\Delta(1+z)] = \log_{10}[\Delta(\nu/\nu_{\text{obs}})] = 0.1$  (where  $\nu$  is the rest frame frequency), with the corresponding effective redshift located in the center of the frequency bin. This results in four bins for the SPHEREx H $\alpha$  observations (with effective redshifts  $z = \{0.55, 1.90, 3.20, 4.52\}$ ) and three bins for the Lyman- $\alpha$  line ( $z = \{5.74, 7.01, 8.78\}$ ); a single redshift bin for COMAP at  $z = 2.84$ , and five redshift bins for the IMS3 CO experiment ( $z = \{2.73, 4.01, 5.30, 6.58, 7.87\}$ ).

Following Ref. [14], we apply the Fisher matrix formalism [26, 27] to forecast constraints on the BAO measurements using the LIM power spectrum multipoles up to the hexadecapole. We take the fiducial values for the  $\Lambda$ CDM model parameters from the best fit to the combination of the full CMB Planck dataset and BAO from SDSS galaxies [7, 10]. Finally, we use the halo mass function and halo bias fitting function introduced in Ref. [28].

In table II, we report forecasted marginalized 68% confidence-level relative constraints on  $D_A(z)/r_s$  and  $H(z)r_s$  from the surveys considered. In Fig. 1, we compare them with existing [10, 29–31] and prospective [32] measurements from galaxy surveys. Due to its poor spectral resolution, SPHEREx constraints on  $H(z)r_s$  are expected to be very weak. However, SPHEREx will provide constraints on  $D_A(z)/r_s$  of  $\sim 3\%$ – $5\%$  precision almost up to  $z = 5$ . This is not the case for COMAP, whose power to constrain  $D_A(z)/r_s$  and  $H(z)r_s$  is more balanced. While COMAP1 will be less precise, both COMAP2, with a precision of  $\sim 5\%$ – $6\%$ , and SPHEREx (only in the transverse direction) will be competitive with existing measurements, and not fall much behind of DESI [32].

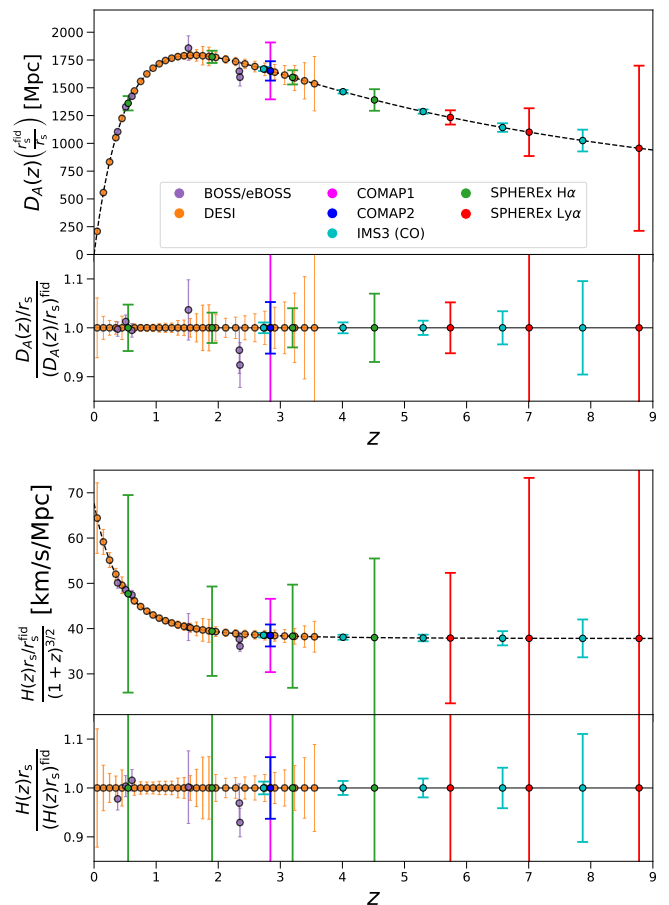


FIG. 1: 68% confidence-level marginalized current and forecasted constraints on the angular diameter distance (top) and Hubble expansion rate over  $(1+z)^{3/2}$  (bottom) as a function of redshift, weighted by the ratio between the actual sound horizon at radiation drag and its fiducial value. Estimated constraints from LIM observations of H $\alpha$  (green) and Lyman- $\alpha$  (red) lines using SPHEREx, and of CO using COMAP1 (pink), COMAP2 (blue) and IMS3 (cyan) are compared with existing and upcoming measurements from galaxy surveys.

Meanwhile, a future IMS3 (CO) experiment would yield percent-level precision at  $2.7 \lesssim z \lesssim 5.5$ , degrading to  $\sim 3\%$ – $4\%$  at  $z = 6.58$ , and  $\sim 10\%$  at  $z = 7.87$ . The next generation of LIM experiments will thus allow a precise determination of the expansion rate of the Universe up to the epoch of reionization. The first redshift bin would overlap with BAO measurements from the Lyman- $\alpha$  forest observed with galaxy surveys, allowing a calibration of the LIM BAO. Note that the Lyman- $\alpha$  Forest is inherently more sensitive to the radial direction, while the opposite is often true for LIM experiments.

In Figure 2, we show the forecasted marginalized constraints on the plane  $D_A(1+z)^2 - H/(1+z)^{3/2}$ , for the case of CO. The correlation between radial and transverse BAO measurements changes with redshift, although this is mainly driven by the transformation of angular and radial resolutions into physical distances. The correla-

$z$	SPHx (H $\alpha$ )				SPHx (Ly $\alpha$ )			COMAP1	COMAP2	IMS3 (CO)				
	0.55	1.90	3.20	4.52	5.74	7.01	8.78	2.84	2.84	2.73	4.01	5.30	6.58	7.87
$\sigma_{\text{rel}}(D_A(z)/r_s)\%$	4.7	3.1	4.0	7.0	5.2	19.5	77.7	15.4	5.2	1.1	1.1	1.5	3.4	9.5
$\sigma_{\text{rel}}(H(z)r_s)\%$	45.7	25.0	29.7	46.0	38.0	93.6	-	21.0	6.3	1.3	1.4	1.9	4.1	11.0

TABLE II: Forecasted 68% confidence-level marginalized relative constraints on  $D_A(z)/r_s$  and  $H(z)r_s$  from SPHEREx (H $\alpha$ , Lyman- $\alpha$ ), COMAP1 and COMAP2 (CO) and IMS3 (CO) observations (expressed in percentages). We emphasize that measurements of different line emissions are complementary, and when combined they may lead to tighter overall constraints.

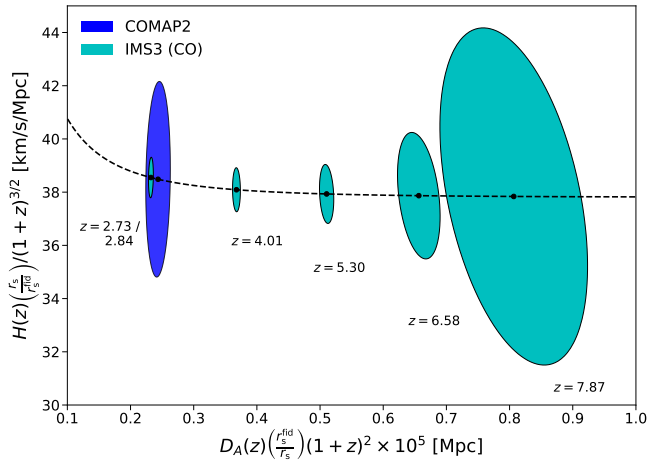


FIG. 2: 68% confidence-level marginalized forecasted constraints on the plane  $D_A(1+z)^2 - H/(1+z)^{3/2}$ , when both are weighted by the ratio between the actual sound horizon at radiation drag and its fiducial value. We show forecasts for the CO line using COMAP2 (blue) and IMS3 (cyan).

tions between cosmological parameters constrained using BAO measurements, such as the Hubble constant  $H_0$  and the matter density parameter today  $\Omega_M$  also change with redshift (see e.g. Ref. [33] for results from galaxy surveys).

It should be emphasized that although the evolution of  $H(z)$  at  $3 \lesssim z \lesssim 10$  is completely determined by  $\Omega_M$  under  $\Lambda$ CDM, we still lack direct empirical evidence of the expansion history in these epochs (CMB lensing provides an integrated constrained, roughly peaked at  $z \sim 2$  [34]). There are models that predict other behaviors, including modified gravity theories or dark matter decaying into lighter dark particles (see e.g. Refs. [35, 36]). These models, as well as alternative modifications of the cosmic expansion in the matter dominated era, could potentially reduce the Hubble tension. Still, model-independent reconstructions of the Hubble parameter currently remain unconstrained beyond  $z \sim 0.7$  [9, 37, 38].

Therefore, perhaps the most convincing way to demonstrate the potential of LIM BAO measurements is to consider a model-independent expansion history. Following Ref. [9], we parametrize  $H(z)$  with natural cubic splines. We locate the nodes of the splines at  $z = \{0.0, 0.2, 0.6, 1.6, 2.4, 4.0, 6.5, 9.0\}$  and fit the values of  $H(z)$  at these nodes using uniform priors and the fol-

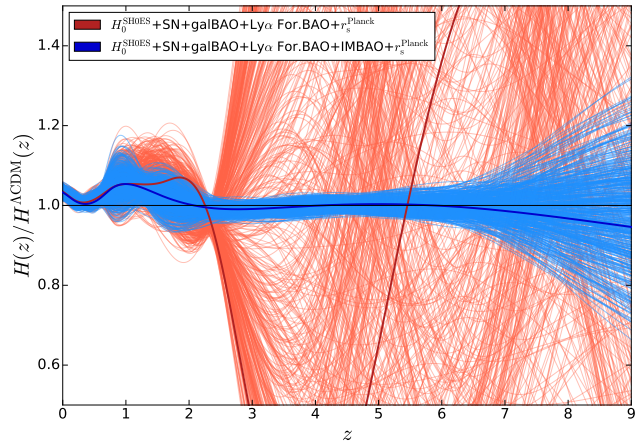


FIG. 3: Constraints on the model independent reconstruction of  $H(z)$  using existing data (red) and including the LIM BAO (blue). We show the best fit with wide solid lines, and 500 random samples drawn from the 68% confidence-level region using thin solid lines.

lowing data<sup>2</sup>: the local measurement of  $H_0$  [6]; Type-Ia supernovae (SNeIa) [11]; BAO from galaxies [10, 40–43], quasars [29] and the Lyman- $\alpha$  forest [30, 31]; and  $r_s$  measured from 2018 Planck data [7]. In addition, we draw samples from the 2D-Gaussian forecasted uncertainties for LIM BAO from SPHEREx and IMS3 (CO), centered at the fiducial values. The node locations are chosen to optimize the constraining power of the different datasets.

In Fig. 3, we show the constraints on the model-independent reconstruction of  $H(z)$ , with and without the estimated LIM BAO measurements. While the  $H_0$  and  $r_s$  measurements constrain the amplitude of  $H(z)$ , the shape is constrained by the SNeIa and BAO data. We can see how, without the LIM BAO measurements, the expansion history is completely unconstrained beyond  $z \sim 2.4$ , given the lack of observations. Fortunately, LIM BAO measurements will enable us to fill this gap and extend the constraints on the expansion history of the Universe up to  $z \sim 9$ . Moreover, in the redshift range  $3 \lesssim z \lesssim 7$ , these constraints will be below the  $\sim 2\% - 3\%$

<sup>2</sup> We run MonteCarlo Markov Chains using the python package `emcee` [39], publicly available at [dfm.io/emcee/](http://dfm.io/emcee/).

level, even for model-independent parametrizations.

Results using our methodology as forecasted in this *Letter* would represent an incredible achievement for cosmology and provide a unique means to directly measure how the Universe expands at  $z \sim 3 - 5$  and up to  $z \sim 7 - 9$ . In the future, standard sirens [44–46] might also achieve this goal, although the sensitivity needed to obtain precise measurements of neutron star mergers and their electromagnetic counterparts at these redshifts is considerably more exigent than what is expected from upcoming and future experiments. Moreover, also using LIM observations, measurements of the velocity-induced acoustic oscillations [47] at cosmic dawn, as proposed in Ref. [48], can potentially constrain the expansion rate at  $15 \lesssim z \lesssim 20$ . Thus, thanks to LIM experiments, our ignorance about the expansion of the Universe may be limited to  $20 \lesssim z \lesssim 1000$ , where there is little room to accommodate a solution to the  $H_0$  tension. LIM can thus shed light on various potential scenarios suggested to solve the tension [49–61].

Foregrounds and line-interlopers might degrade the results reported here, but we emphasize that spectral lines related to star formation are significantly brighter than the 21cm line in comparison to their sources of contamination. Moreover, in the coming years there will be

several LIM observations which will overlap with galaxy surveys. Cross-correlations between different tracers will make it possible to subtract this contamination from the LIM signals (see e.g., Refs. [16, 62]). Finally, we must emphasize that the luminosity functions of spectral lines at high redshift are still highly uncertain. Although using our methodology to disentangle between astrophysical and cosmological dependences, this should not bias the measurements [14], it may certainly affect the precision of the measurement by modifying the signal-to-noise ratio if the amplitude of the LIM power spectrum turns out to be lower than assumed here. We have accounted for this by choosing line emission models whose predictions are neither too optimistic nor too conservative.

To conclude, LIM experiments can provide precise and robust measurements of the BAO scale up to the epoch of reionization at  $z \lesssim 9$ . These observations will provide superb constraints on the expansion history of the Universe, probe models of exotic dark matter, dynamical dark energy, modified gravity, etc., and in general open a new discovery space in the high-redshift universe.

We acknowledge useful conversations with Tzu-Ching Chang, Olivier Doré, Héctor Gil-Marín and Licia Verde. JLB is supported by the Spanish MINECO under grant BES-2015-071307, co-funded by the ESF.

- 
- [1] E. Hubble, “A Relation between Distance and Radial Velocity among Extra-Galactic Nebulae,” *Proceedings of the National Academy of Science* **15** (Mar., 1929) 168–173.
- [2] A. G. Riess, A. V. Filippenko, P. Challis, A. Clocchiatti, A. Diercks, et al., “Observational Evidence from Supernovae for an Accelerating Universe and a Cosmological Constant,” *Astronom. J.* **116** no. 3, (Sep, 1998) 1009–1038, [arXiv:astro-ph/9805201](#) [[astro-ph](#)].
- [3] S. Perlmutter, , and T. S. C. Project, “Measurements of  $\Omega$  and  $\Lambda$  from 42 High-Redshift Supernovae,” *Astrophys. J.* **517** no. 2, (Jun, 1999) 565–586, [arXiv:astro-ph/9812133](#) [[astro-ph](#)].
- [4] A. J. Cuesta, L. Verde, A. Riess, and R. Jimenez, “Calibrating the cosmic distance scale ladder: the role of the sound horizon scale and the local expansion rate as distance anchors,” *Mon. Not. Roy. Astron. Soc.* **448** no. 4, (2015) 3463–3471, [arXiv:1411.1094](#) [[astro-ph.CO](#)].
- [5] W. L. Freedman, “Cosmology at a Crossroads,” *Nat. Astron.* **1** (2017) 0121, [arXiv:1706.02739](#) [[astro-ph.CO](#)].
- [6] A. G. Riess, S. Casertano, W. Yuan, L. M. Macri, and D. Scolnic, “Large Magellanic Cloud Cepheid Standards Provide a 1% Foundation for the Determination of the Hubble Constant and Stronger Evidence for Physics Beyond LambdaCDM,” [arXiv e-prints](#) (Mar., 2019) , [arXiv:1903.07603](#).
- [7] Planck Collaboration, N. Aghanim, et al., “Planck 2018 results. VI. Cosmological parameters,” [ArXiv e-prints](#) (July, 2018) , [arXiv:1807.06209](#).
- [8] K. C. Wong et al., “H0LiCOW XIII. A 2.4% measurement of  $H_0$  from lensed quasars: 5.3 $\sigma$  tension between early and late-Universe probes,” [arXiv:1907.04869](#) [[astro-ph.CO](#)].
- [9] J. L. Bernal, L. Verde, and A. G. Riess, “The trouble with  $H_0$ ,” *JCAP* **10** (Oct., 2016) 019, [arXiv:1607.05617](#).
- [10] **SDSS-III BOSS** Collaboration, S. Alam and et al., “The clustering of galaxies in the completed SDSS-III Baryon Oscillation Spectroscopic Survey: cosmological analysis of the DR12 galaxy sample,” *MNRAS* **470** (Sept., 2017) 2617–2652, [arXiv:1607.03155](#).
- [11] D. M. Scolnic, D. O. Jones, A. Rest, Y. C. Pan, et al., “The Complete Light-curve Sample of Spectroscopically Confirmed SNe Ia from Pan-STARRS1 and Cosmological Constraints from the Combined Pantheon Sample,” *Astrophys. J.* **859** no. 2, (Jun, 2018) 101, [arXiv:1710.00845](#) [[astro-ph.CO](#)].
- [12] E. D. Kovetz, M. P. Viero, A. Lidz, L. Newburgh, M. Rahman, E. Switzer, M. Kamionkowski, et al., “Line-Intensity Mapping: 2017 Status Report,” [arXiv e-prints](#) (Sep, 2017) [arXiv:1709.09066](#), [arXiv:1709.09066](#) [[astro-ph.CO](#)].
- [13] K. S. Karkare and S. Bird, “Constraining the Expansion History and Early Dark Energy with Line Intensity Mapping,” *Phys. Rev.* **D98** no. 4, (2018) 043529, [arXiv:1806.09625](#) [[astro-ph.CO](#)].
- [14] J. L. Bernal, P. C. Breyse, H. Gil-Marín, and E. D. Kovetz, “A User’s Guide to Extracting Cosmological Information from Line-Intensity Maps,” *In preparation* (2019) .
- [15] C. Alcock and B. Paczynski, “An evolution free test for

- non-zero cosmological constant,” *Nature* **281** (Oct, 1979) 358.
- [16] M. B. Silva, M. G. Santos, Y. Gong, A. Cooray, and J. Bock, “Intensity Mapping of Ly $\alpha$  Emission during the Epoch of Reionization,” *ApJ* **763** no. 2, (Feb, 2013) 132, [arXiv:1205.1493 \[astro-ph.CO\]](#).
- [17] Y. Gong, A. Cooray, M. B. Silva, M. Zemcov, C. Feng, M. G. Santos, O. Dore, and X. Chen, “Intensity Mapping of H $\alpha$ , H $\beta$ , [OII], and [OIII] Lines at  $z < 5$ ,” *ApJ* **835** no. 2, (Feb, 2017) 273, [arXiv:1610.09060 \[astro-ph.GA\]](#).
- [18] T. Y. Li, R. H. Wechsler, K. Devaraj, and S. E. Church, “Connecting CO Intensity Mapping to Molecular Gas and Star Formation in the Epoch of Galaxy Assembly,” *Astrophys. J.* **817** (Feb., 2016) 169, [arXiv:1503.08833 \[astro-ph.CO\]](#).
- [19] A. Lidz, S. R. Furlanetto, S. P. Oh, J. Aguirre, T.-C. Chang, O. Dore, and J. R. Pritchard, “Intensity Mapping with Carbon Monoxide Emission Lines and the Redshifted 21 cm Line,” *Astrophys. J.* **741** (2011) 70, [arXiv:1104.4800 \[astro-ph.CO\]](#).
- [20] P. C. Breysse, E. D. Kovetz, and M. Kamionkowski, “Carbon Monoxide Intensity Mapping at Moderate Redshifts,” *Mon. Not. Roy. Astron. Soc.* **443** no. 4, (2014) 3506–3512, [arXiv:1405.0489 \[astro-ph.CO\]](#).
- [21] P. C. Breysse and R. M. Alexandroff, “Observing AGN feedback with CO intensity mapping,” *arXiv e-prints* (Apr, 2019) [arXiv:1904.03197](#), [arXiv:1904.03197 \[astro-ph.GA\]](#).
- [22] O. Doré, J. Bock, M. Ashby, P. Capak, A. Cooray, et al., “Cosmology with the SPHEREX All-Sky Spectral Survey,” *arXiv e-prints* (Dec, 2014) [arXiv:1412.4872](#), [arXiv:1412.4872 \[astro-ph.CO\]](#).
- [23] K. Cleary, M.-A. Bigot-Sazy, D. Chung, et al., “The CO Mapping Array Pathfinder (COMAP),” in *AAS Meeting Abstracts #227*, vol. 227, p. 426.06. Jan., 2016.
- [24] R. M. Prestage, “The Green Bank Telescope,” in *SPIE Conference Series*, vol. 6267, p. 626712. Jun, 2006.
- [25] E. J. Murphy, “A next-generation Very Large Array,” in *Astrophysical Masers: Unlocking the Mysteries of the Universe*, A. Tarchi, M. J. Reid, and P. Castangia, eds., vol. 336 of *IAU Symposium*, pp. 426–432. Aug, 2018. [arXiv:1711.09921 \[astro-ph.IM\]](#).
- [26] R. A. Fisher, “The Fiducial Argument in Statistical Inference,” *Annals Eugen.* **6** (1935) 391–398.
- [27] M. Tegmark, A. N. Taylor, and A. F. Heavens, “Karhunen-Loève Eigenvalue Problems in Cosmology: How Should We Tackle Large Data Sets?,” *Astrophys. J.* **480** (May, 1997) 22–35, [astro-ph/9603021](#).
- [28] J. L. Tinker, B. E. Robertson, A. V. Kravtsov, A. Klypin, M. S. Warren, G. Yepes, and S. Gottlöber, “The Large-scale Bias of Dark Matter Halos: Numerical Calibration and Model Tests,” *ApJ* **724** no. 2, (Dec, 2010) 878–886, [arXiv:1001.3162 \[astro-ph.CO\]](#).
- [29] H. Gil-Marín, J. Guy, P. Zarrouk, E. Burtin, C.-H. Chuang, and W. J. o. Percival, “The clustering of the SDSS-IV extended Baryon Oscillation Spectroscopic Survey DR14 quasar sample: structure growth rate measurement from the anisotropic quasar power spectrum in the redshift range  $0.8 < z < 2.2$ ,” *MNRAS* **477** (June, 2018) 1604–1638, [arXiv:1801.02689](#).
- [30] V. de Sainte Agathe, C. Balland, H. du Mas des Bourboux, N. G. Busca, M. Blomqvist, J. Guy, J. Rich, A. Font-Ribera, M. M. Pieri, J. E. Bautista, K. Dawson, J.-M. Le Goff, A. de la Macorra, N. Palanque-Delabrouille, W. J. Percival, I. Pérez-Ràfols, D. P. Schneider, A. Slosar, and C. Yèche, “Baryon acoustic oscillations at  $z = 2.34$  from the correlations of Ly $\alpha$  absorption in eBOSS DR14,” *arXiv e-prints* (Apr., 2019) , [arXiv:1904.03400](#).
- [31] M. Blomqvist, H. du Mas des Bourboux, N. G. Busca, V. de Sainte Agathe, J. Rich, C. Balland, J. E. Bautista, K. Dawson, A. Font-Ribera, J. Guy, J.-M. Le Goff, N. Palanque-Delabrouille, W. J. Percival, I. Pérez-Ràfols, M. M. Pieri, D. P. Schneider, A. Slosar, and C. Yèche, “Baryon acoustic oscillations from the cross-correlation of Ly $\alpha$  absorption and quasars in eBOSS DR14,” *arXiv e-prints* (Apr., 2019) , [arXiv:1904.03430](#).
- [32] DESI Collaboration, A. Aghamousa, and et al., “The DESI Experiment Part I: Science, Targeting, and Survey Design,” *ArXiv e-prints* (Oct., 2016) , [arXiv:1611.00036 \[astro-ph.IM\]](#).
- [33] A. Cuceu, J. Farr, P. Lemos, and A. Font-Ribera, “Baryon Acoustic Oscillations and the Hubble Constant: Past, Present and Future,” *arXiv e-prints* (Jun, 2019) [arXiv:1906.11628](#), [arXiv:1906.11628 \[astro-ph.CO\]](#).
- [34] **Planck** Collaboration, N. Aghanim et al., “Planck 2018 results. VIII. Gravitational lensing,” [arXiv:1807.06210 \[astro-ph.CO\]](#).
- [35] M. Raveri, “Reconstructing Gravity on Cosmological Scales,” *arXiv e-prints* (Feb, 2019) [arXiv:1902.01366](#), [arXiv:1902.01366 \[astro-ph.CO\]](#).
- [36] K. Vattis, S. M. Koushiappas, and A. Loeb, “Late universe decaying dark matter can relieve the H $_0$  tension,” *arXiv e-prints* (Mar, 2019) [arXiv:1903.06220](#), [arXiv:1903.06220 \[astro-ph.CO\]](#).
- [37] L. Verde, J. L. Bernal, A. F. Heavens, and R. Jimenez, “The length of the low-redshift standard ruler,” *MNRAS* **467** (May, 2017) 731–736, [arXiv:1607.05297](#).
- [38] S. Joudaki, M. Kaplinghat, R. Keeley, and D. Kirkby, “Model independent inference of the expansion history and implications for the growth of structure,” *Phys. Rev.* **D97** no. 12, (2018) 123501, [arXiv:1710.04236 \[astro-ph.CO\]](#).
- [39] D. Foreman-Mackey, D. W. Hogg, D. Lang, and J. Goodman, “emcee: The MCMC Hammer,” *Publications of the Astronomical Society of the Pacific* **125** (Mar., 2013) 306–312, [arXiv:1202.3665 \[astro-ph.IM\]](#).
- [40] F. Beutler, C. Blake, M. Colless, D. H. Jones, L. Staveley-Smith, L. Campbell, Q. Parker, W. Saunders, and F. Watson, “The 6dF Galaxy Survey: baryon acoustic oscillations and the local Hubble constant,” *Mon. Not. Roy. Astron. Soc.* **416** (Oct., 2011) 3017–3032, [arXiv:1106.3366](#).
- [41] A. J. Ross, L. Samushia, C. Howlett, W. J. Percival, A. Burden, and M. Manera, “The clustering of the SDSS DR7 main Galaxy sample - I. A 4 per cent distance measure at  $z = 0.15$ ,” *Mon. Not. Roy. Astron. Soc.* **449** (May, 2015) 835–847, [arXiv:1409.3242](#).
- [42] E. A. Kazin, J. Koda, C. Blake, N. Padmanabhan, S. Brough, M. Colless, C. Contreras, W. Couch, S. Croom, D. J. Croton, T. M. Davis, M. J. Drinkwater, K. Forster, D. Gilbank, M. Gladders, K. Glazebrook, B. Jelliffe, R. J. Jurek, I.-h. Li, B. Madore, D. C.

- Martin, K. Pimblett, G. B. Poole, M. Pracy, R. Sharp, E. Wisnioski, D. Woods, T. K. Wyder, and H. K. C. Yee, “The WiggleZ Dark Energy Survey: improved distance measurements to  $z = 1$  with reconstruction of the baryonic acoustic feature,” *Mon. Not. Roy. Astron. Soc.* **441** (July, 2014) 3524–3542, [arXiv:1401.0358](#).
- [43] J. E. Bautista et al., “The SDSS-IV extended Baryon Oscillation Spectroscopic Survey: Baryon Acoustic Oscillations at redshift of 0.72 with the DR14 Luminous Red Galaxy Sample,” *ArXiv e-prints* (Dec., 2017), [arXiv:1712.08064](#).
- [44] B. P. Abbott, R. Abbott, T. D. Abbott, F. Acernese, K. Ackley, C. Adams, T. Adams, P. Addesso, R. X. Adhikari, V. B. Adya, and et al., “A gravitational-wave standard siren measurement of the Hubble constant,” *ArXiv e-prints* (Oct., 2017), [arXiv:1710.05835](#).
- [45] S. M. Feeney, H. V. Peiris, A. R. Williamson, S. M. Nissanke, D. J. Mortlock, J. Alsing, and D. Scolnic, “Prospects for resolving the Hubble constant tension with standard sirens,” *Phys. Rev. Lett.* **122** no. 6, (2019) 061105, [arXiv:1802.03404 \[astro-ph.CO\]](#).
- [46] H.-Y. Chen, M. Fishbach, and D. E. Holz, “A two per cent Hubble constant measurement from standard sirens within five years,” *Nature* **562** no. 7728, (2018) 545–547, [arXiv:1712.06531 \[astro-ph.CO\]](#).
- [47] J. B. Muñoz, “Velocity-induced Acoustic Oscillations at Cosmic Dawn,” *arXiv e-prints* (Apr, 2019) [arXiv:1904.07881](#), [arXiv:1904.07881 \[astro-ph.CO\]](#).
- [48] J. B. Muñoz, “A Standard Ruler at Cosmic Dawn,” *arXiv e-prints* (Apr, 2019) [arXiv:1904.07868](#), [arXiv:1904.07868 \[astro-ph.CO\]](#).
- [49] T. Karwal and M. Kamionkowski, “Dark energy at early times, the Hubble parameter, and the string axiverse,” *Phys. Rev.* **D94** no. 10, (2016) 103523, [arXiv:1608.01309 \[astro-ph.CO\]](#).
- [50] V. Poulin, T. L. Smith, T. Karwal, and M. Kamionkowski, “Early Dark Energy Can Resolve The Hubble Tension,” *arXiv e-prints* (Nov, 2018) [arXiv:1811.04083](#), [arXiv:1811.04083 \[astro-ph.CO\]](#).
- [51] M.-X. Lin, G. Benevento, W. Hu, and M. Raveri, “Acoustic Dark Energy: Potential Conversion of the Hubble Tension,” [arXiv:1905.12618 \[astro-ph.CO\]](#).
- [52] C. D. Kreisch, F.-Y. Cyr-Racine, and O. Doré, “The Neutrino Puzzle: Anomalies, Interactions, and Cosmological Tensions,” *arXiv e-prints* (Feb, 2019) [arXiv:1902.00534](#), [arXiv:1902.00534 \[astro-ph.CO\]](#).
- [53] W. Yang, S. Pan, S. Vagnozzi, E. Di Valentino, D. F. Mota, and S. Capozziello, “Dawn of the dark: unified dark sectors and the EDGES Cosmic Dawn 21-cm signal,” [arXiv:1907.05344 \[astro-ph.CO\]](#).
- [54] M. Archidiacono, D. C. Hooper, R. Murgia, S. Bohr, J. Lesgourgues, and M. Viel, “Constraining Dark Matter – Dark Radiation interactions with CMB, BAO, and Lyman- $\alpha$ ,” [arXiv:1907.01496 \[astro-ph.CO\]](#).
- [55] D. Hooper, G. Krnjaic, and S. D. McDermott, “Dark Radiation and Superheavy Dark Matter from Black Hole Domination,” [arXiv:1905.01301 \[hep-ph\]](#).
- [56] K. Vattis, S. M. Koushiappas, and A. Loeb, “Dark matter decaying in the late Universe can relieve the  $H_0$  tension,” *Phys. Rev.* **D99** no. 12, (2019) 121302, [arXiv:1903.06220 \[astro-ph.CO\]](#).
- [57] K. L. Pandey, T. Karwal, and S. Das, “Alleviating the  $H_0$  and  $\sigma_8$  anomalies with a decaying dark matter model,” [arXiv:1902.10636 \[astro-ph.CO\]](#).
- [58] S. Pan, W. Yang, E. Di Valentino, E. N. Saridakis, and S. Chakraborty, “Interacting scenarios with dynamical dark energy: observational constraints and alleviation of the  $H_0$  tension,” [arXiv:1907.07540 \[astro-ph.CO\]](#).
- [59] H. Desmond, B. Jain, and J. Sakstein, “A local resolution of the Hubble tension: The impact of screened fifth forces on the cosmic distance ladder,” [arXiv:1907.03778 \[astro-ph.CO\]](#).
- [60] P. Agrawal, F.-Y. Cyr-Racine, D. Pinner, and L. Randall, “Rock ‘n’ Roll Solutions to the Hubble Tension,” [arXiv:1904.01016 \[astro-ph.CO\]](#).
- [61] S. Vagnozzi, “New physics in light of the  $H_0$  tension: an alternative view,” [arXiv:1907.07569 \[astro-ph.CO\]](#).
- [62] G. Sun, L. Monceli, M. P. Viero, M. B. Silva, J. Bock, C. M. Bradford, T. C. Chang, Y. T. Cheng, A. R. Cooray, A. Crites, S. Hailey-Dunsheath, B. Uzgil, J. R. Hunacek, and M. Zemcov, “A Foreground Masking Strategy for [C II] Intensity Mapping Experiments Using Galaxies Selected by Stellar Mass and Redshift,” *Astrophys. J.* **856** no. 2, (Apr, 2018) 107, [arXiv:1610.10095 \[astro-ph.GA\]](#).